

- Bradshaw, M. F. & Cumming, B. G. The direction of retinal motion facilitates binocular stereopsis. *Proc. R. Soc. Lond. B* **264**, 1421–1427 (1997).
- Mayhew, J. E. & Frisby, J. P. Stereopsis masking in humans is not orientationally tuned. *Perception* **7**, 431–436 (1978).
- Mansfield, J. S. & Parker, A. J. An orientation-tuned component in the contrast masking of stereopsis. *Vision Res.* **33**, 1535–1544 (1993).
- Rogers, B. J. & Graham, M. E. Similarities between motion parallax and stereopsis in human depth perception. *Vision Res.* **22**, 261–270 (1982).
- Bradshaw, M. F. & Rogers, B. J. The interaction of binocular disparity and motion parallax in the computation of depth. *Vision Res.* **36**, 3457–3468 (1996).
- Tittle, J. S. & Braunstein, M. L. Recovery of 3-D shape from binocular disparity and structure from motion. *Percept. Psychophys.* **54**, 157–169 (1993).
- Richards, W. Structure from stereo and motion. *J. Opt. Soc. Am. A* **2**, 343–349 (1985).
- Landy, M. S., Maloney, L. T., Johnston, E. B. & Young, M. Measurement and modeling of depth cue combination: in defense of weak fusion. *Vision Res.* **35**, 389–412 (1995).
- Julesz, B. *Foundations of Cyclopean Perception* (Univ. Chicago Press, Chicago, 1971).

Acknowledgements

R.v.E. was supported by a NIH grant awarded to B.A. and by the Royal Netherlands Academy of Arts and Sciences, and B.A. was supported in part by NIH.

Correspondence and requests for materials should be addressed to B.L.A. (e-mail: bart@mit.edu).

The homeobox gene *lim-6* is required for distinct chemosensory representations in *C. elegans*

Jonathan T. Pierce-Shimomura, Serge Faumont, Michelle R. Gaston, Bret J. Pearson & Shawn R. Lockery

Institute of Neuroscience, 1254 University of Oregon, Eugene, Oregon 97403, USA

The ability to discriminate between different chemical stimuli is crucial for food detection, spatial orientation and other adaptive behaviours in animals. In the nematode *Caenorhabditis elegans*, spatial orientation in gradients of soluble chemoattractants (chemotaxis) is controlled mainly by a single pair of chemosensory neurons¹. These two neurons, ASEL and ASER, are left–right homologues in terms of the disposition of their somata and processes, morphology of specialized sensory endings, synaptic partners and expression profile of many genes^{2,3}. However, recent gene-expression studies have revealed unexpected asymmetries between ASEL and ASER. ASEL expresses the putative receptor guanylyl cyclase genes *gcy-6* and *gcy-7*, whereas ASER expresses *gcy-5* (ref. 4). In addition, only ASEL expresses the homeobox gene *lim-6*, an orthologue of the human *LMX1* subfamily of homeobox genes⁵. Here we show, using laser ablation of neurons and whole-cell patch-clamp electrophysiology, that the asymmetries between ASEL and ASER extend to the functional level. ASEL is primarily sensitive to sodium, whereas ASER is primarily sensitive to chloride and potassium. Furthermore, we find that *lim-6* is required for this functional asymmetry and for the ability to distinguish sodium from chloride. Thus, a homeobox gene increases the representational capacity of the nervous system by establishing asymmetric functions in a bilaterally symmetrical neuron pair.

To determine whether *C. elegans* can distinguish between the attractants sodium and chloride in our experimental system⁶, we performed a discrimination test in which we examined the chemotaxis performance of worms in a gradient of sodium (50 μM to 10 mM) superimposed on a saturating background concentration of chloride (100 mM), and vice versa (Fig. 1a, d). In both cases, worms migrated toward the peak of the gradient as expected⁷,

although the overall chemotaxis performance was reduced relative to control worms tested in sodium or chloride gradients but with no background ion concentration (Fig. 1b, d).

However, the chemotaxis performance of worms tested under conditions in which the gradient and background concentration contained the same ion (Fig. 1c, d) degenerated to roughly chance level, defined as the chemotaxis performance of worms tested in the absence of a gradient (Fig. 1d, dotted line). Together, these results show that sodium chemotaxis persists against a background of

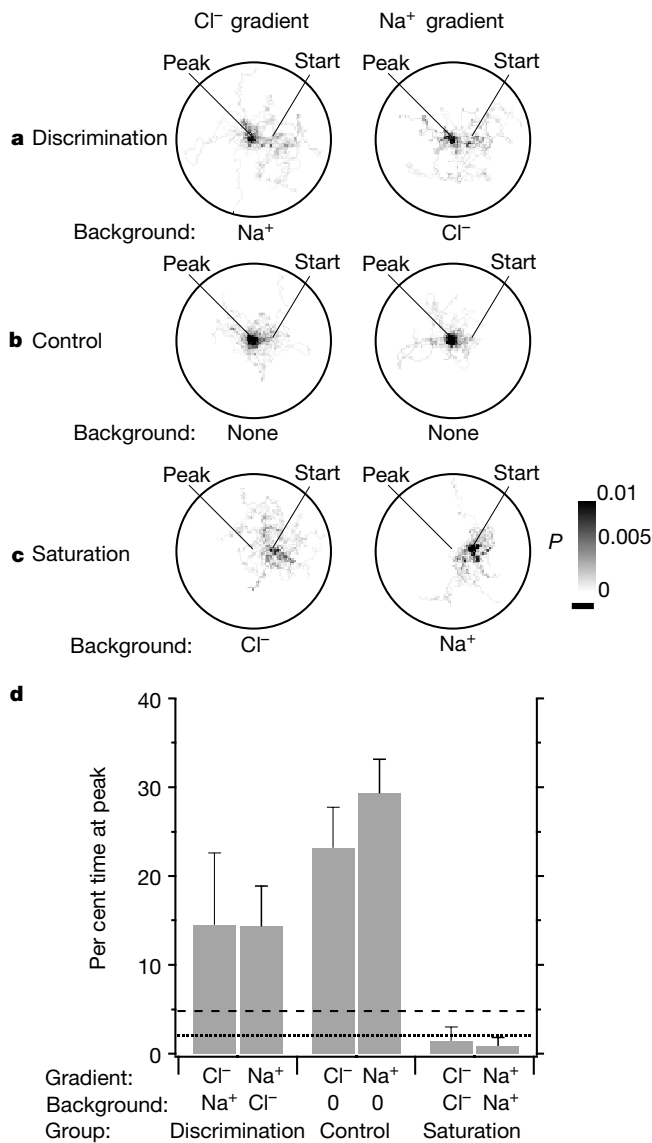


Figure 1 Discrimination of sodium and chloride by wild-type *C. elegans*. **a–c**, Probability density plots for worms assayed in gradients of chloride (left) and sodium (right) originating at the centre of the plate (peak), *n* ≥ 15. Grey scale indicates the probability per unit area of finding a worm at a given location in the plate during the 20-min assay. Scale bar, 1 cm. **a**, Discrimination. Worms located and remained at the peak of a chloride gradient superimposed on a high background concentration (100 mM) of sodium, or at the peak of a sodium gradient superimposed on a high background concentration (100 mM) of chloride. **b**, Control. Chemotaxis performance was normal in gradients identical to those in **a** when the background ion was omitted. **c**, Saturation. Worms failed to locate the peak of the gradient when it was superimposed on a high background concentration (100 mM) of the same ion. **d**, Average per cent time spent at the gradient peak for worms in the six conditions shown in **a–c**. Dotted line indicates mean chance performance, measured by assaying 74 worms in plates with neither gradient nor background. Dashed line indicates upper 95 per cent confidence limit for mean chance performance.

chloride sufficient to saturate the chloride response, and chloride chemotaxis persists against a background of sodium sufficient to saturate the sodium response. Thus, *C. elegans* has distinct sensory pathways for detecting sodium and chloride ions, in agreement with previous qualitative observations⁷.

To identify the neuronal constituents of these two sensory pathways, we compared the effects on chloride and sodium chemotaxis of unilateral ablations of the ASE neurons (Fig. 2a, b). We found that chloride chemotaxis was disrupted by ablation of ASER, indicating that it is a necessary constituent of the chloride sensory pathway. In contrast, chloride chemotaxis was unaffected by ablation of ASEL, suggesting that ASEL is not a necessary constituent of the chloride pathway. Furthermore, we found that sodium chemotaxis was disrupted by ablation of ASEL, indicating that it is a necessary constituent of the sodium sensory pathway. Although ablation of ASER had little or no effect on sodium chemotaxis, the effect of bilateral ablation of the ASE neurons was greater than the effect of unilateral ablation of ASEL (Bonferroni post hoc comparison, $P < 0.001$). Thus, ASER seems to be a secondary constituent of the sodium pathway. We conclude that the asymmetries in gene expression in the ASE neurons coincide with differences in sensory function.

As the strongest unilateral ablation effects were for ASEL in the case of sodium chemotaxis and ASER in the case of chloride chemotaxis, we thought that ASEL and ASER might be specialized for detection of cations and anions, respectively. Therefore, we compared the effects of unilateral and bilateral ablation of ASE neurons on potassium chemotaxis as an example of a response to a second cation (Fig. 2c). We found that potassium chemotaxis was disrupted by ablation of ASER, but not by ablation of ASEL, indicating that ASER is a necessary constituent of the potassium pathway, but ASEL is not. Thus, ASER is not specialized for detecting anions, and the functional asymmetries between ASEL and ASER extend to a third ion.

The ablation data are summarized in Fig. 2d, which shows the respective contribution of the ASE neurons to the sodium, chloride and potassium pathways. (The three other chemosensory neuron pairs known to be necessary for normal chemotaxis to sodium and chloride ions—ADF, ASG and ASI—were not tested because their joint contribution to chemotaxis is much less than that of the ASE neurons¹.) Only ASER contributes to the chloride and potassium pathways. Both ASER and ASEL contribute to the sodium pathway, but the latter makes the stronger contribution.

Our finding that ASEL, the main constituent of the sodium pathway, is not part of the potassium pathway suggests that sodium chemotaxis should persist against a high background of potassium—a prediction at odds with previous work⁷. In our more quantitative behavioural assay, however, sodium chemotaxis persists against a background of 100 mM potassium (per cent time at peak: Na^+ gradient with K^+ background, 20.7 ± 6.02 , $n = 18$, versus no gradient, 1.97 ± 1.02 , $n = 74$; $t = 6.02$, $P < 0.0001$). We did, however, observe a substantial reduction in potassium chemotaxis against a background of 100 mM sodium (per cent time at peak: K^+ gradient with Na^+ background, 8.37 ± 5.35 , $n = 33$; K^+ gradient with no background, 23.1 ± 5.67 , $n = 15$; $t = 3.91$, $P < 0.001$), consistent with previous results⁷ and our finding that the potassium pathway and the secondary sodium pathway converge on ASER.

To determine whether the differences between ASEL and ASER in sensory function are reflected in their electrophysiology, we performed whole-cell voltage-clamp recordings from ASEL for comparison with previous recordings from ASER⁸. Net membrane current evoked by a family of voltage pulses between -154 and $+46$ mV (holding potential = -74 mV) was qualitatively similar in ASEL and ASER (Fig. 3a). Both neurons exhibited a time-independent inward current activated by hyperpolarization below -90 mV, and a fast activating outward current activated by depolarization. Outward current decayed exponentially over time in both neurons.

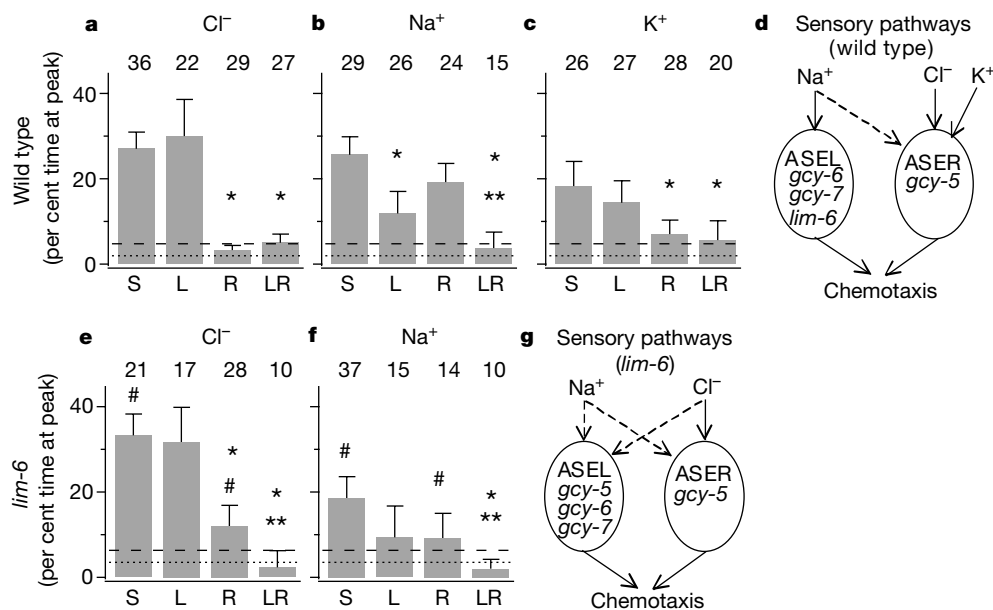


Figure 2 Effect of ablations of ASEL and ASER on chemotaxis performance in chloride, sodium and potassium gradients. **a–c, e, f**, Per cent time at the gradient peak for four groups of worms: unablated sham (S), ASEL ablation (L), ASER ablation (R), and ASEL plus ASER ablation (LR). Single asterisks indicate a significant difference relative to sham ($P < 0.01$); double asterisks indicate a significant difference relative to the ASEL ablation or the ASER ablation ($P < 0.01$); hash indicates a significant difference relative to the same groups in wild-type worms ($P < 0.05$). Numbers above the bars indicate sample sizes. Dotted lines indicate mean chance performance, measured by assaying worms in

plates with neither gradient nor background. Dashed lines indicate the upper 95 per cent confidence limit for chance performance. **d**, Summary of the sodium, chloride, and potassium sensory pathways based on the data in **a–c**. Dashed line indicates that ASER is a secondary constituent of the sodium pathway. **g**, Summary of the sodium and chloride sensory pathways in *lim-6* based on the data in **e** and **f**; the potassium pathway was not tested. Dashed lines indicate weakened or secondary sensory function. The asymmetric function of the ASE neurons is correlated with asymmetric expression of the receptor guanylyl cyclase genes *gcy-5*, *-6* and *-7* and the homeobox gene *lim-6* (refs 4, 5).

Substitution of *N*-methyl-D-glucamine for potassium in the recording pipette abolished outward current in both ASEL (data not shown) and ASER⁸, suggesting that it is carried by potassium ions. Rates of inactivation for outward current vary widely among *C. elegans* neurons⁸. We therefore compared inactivation rates of the outward current at +46 mV for ASER and ASEL. Notably, we found no statistical difference in the time constants of inactivation for ASER (19.7 ± 2.4 ms; $n = 31$) and ASEL (20.8 ± 3.9 ms; $n = 12$, $t = 1.60$, $P > 0.05$), suggesting that the transient current may be carried by the same or similar potassium channels.

Plots of peak current density versus voltage were also strikingly similar for ASEL ($n = 14$) and ASER ($n = 29$) (Fig. 3b, left). The plot of steady-state current density versus voltage, however, revealed that outward current density above -14 mV is increased about 1.5–2-fold in ASEL (Fig. 3b, right; analysis of variance, $P < 0.01$). Thus, the difference in sensory function between ASEL and ASER is reflected in a difference in the amount of outward current generated when the neuron is depolarized, which could in turn produce a difference in the threshold for regenerative events seen in ASE neurons⁸. Whereas the functional consequence of this difference remains to be investigated, the overall electrophysiological similarity of the two neurons suggests that differences in the chemosensitivities of the two neurons to sodium, chloride and potassium, rather than differences in voltage-dependent currents, are responsible for the asymmetrical contributions of ASEL and ASER to chemotaxis.

In the mutant *lim-6(nr2073)*, a putative null missing the homeo-domain and one of two LIM domains of the protein, *gcy-5*, which is normally expressed only in ASER, is also expressed in ASEL⁵. Thus, the *lim-6* gene is required for asymmetric *gcy-5* expression in ASEL and ASER. To determine whether the *lim-6* gene is also required for the asymmetric sensory functions of ASEL and ASER, we compared the effect on chloride chemotaxis of unilateral ablations of ASE neurons in *lim-6* mutants (Fig. 2e). We found that although chloride chemotaxis was reduced by ablation of ASER, the reduction was significantly less than in wild-type worms (Fig. 2e, R, versus Fig. 2a, R: $t = 3.72$, $P < 0.001$). Moreover, *lim-6* mutants in which ASER was ablated performed significantly better than chance (Fig. 2e, R, versus chance: $t = 3.17$, $P < 0.01$), in contrast to wild-type worms in which ASER was ablated (Fig. 2a, R, versus chance: $t = 0.867$, $P > 0.05$). Thus, in *lim-6* mutants, chloride

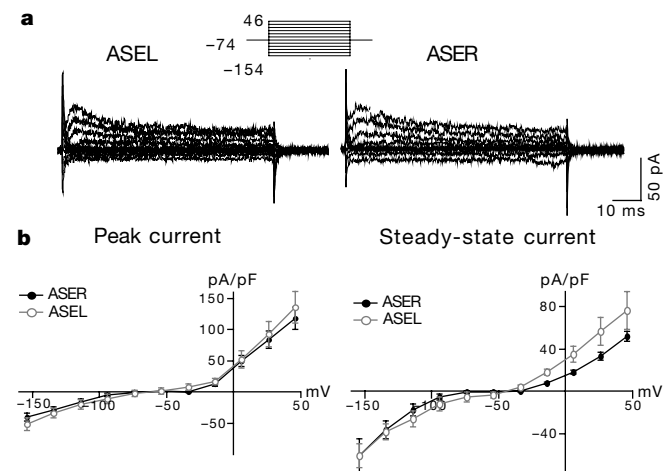


Figure 3 Comparison of membrane currents in ASEL and ASER. **a**, Currents evoked by a family of 80-ms voltage pulses between -154 and +46 mV from a holding potential of -74 mV in ASEL (left) and ASER (right). **b**, Current density versus voltage plots for peak (left) and steady-state current (right) in ASER (filled circles, $n = 29$) and ASEL (open circles, $n = 14$). Steady-state current was calculated as the mean current over the last five milliseconds of the voltage pulse. Bars, 95 per cent confidence intervals.

chemotaxis persists in the absence of ASER, suggesting the existence of a new constituent of the chloride pathway.

A likely candidate for this constituent was ASEL, because it now expressed *gcy-5*, a characteristic feature of the chloride-sensitive ASER neuron. Although killing ASEL had no effect on chloride chemotaxis in *lim-6* mutants, killing ASER together with ASEL reduced chloride chemotaxis more than ablating ASER alone

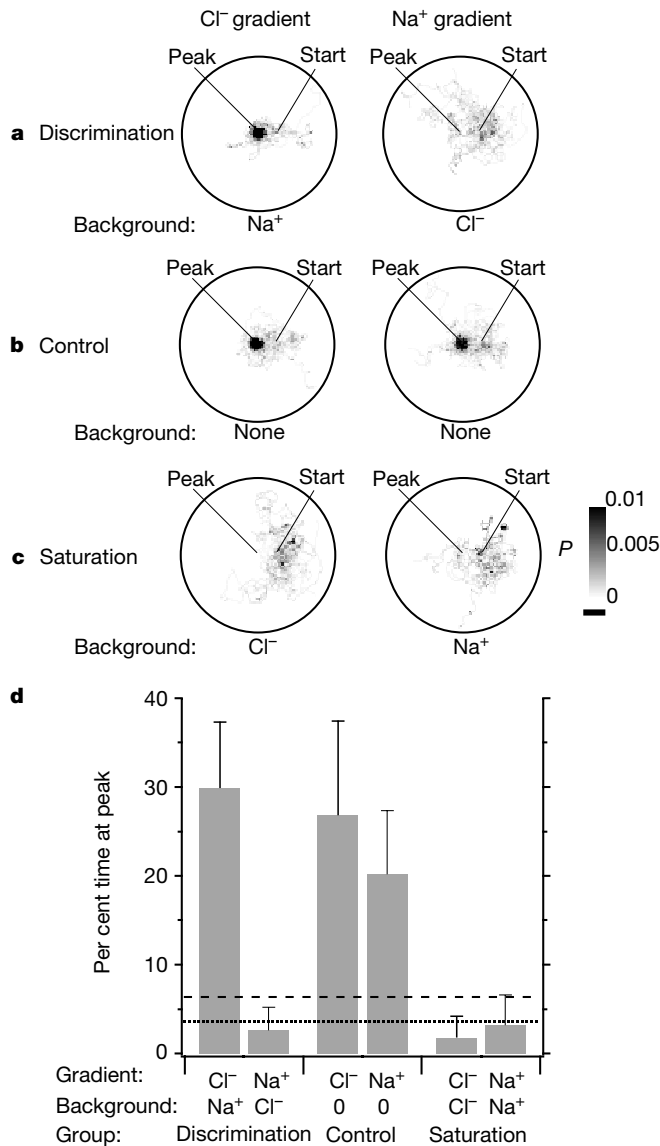


Figure 4 Discrimination of sodium and chloride in *lim-6* mutants. **a–c**, Probability density plots for *lim-6* mutants assayed in gradients of chloride (left) and sodium (right) originating at the centre of the plate (peak) ($n \geq 15$). Grey scale indicates the probability per unit area of finding a worm at a given location in the plate during the 20-min assay. Scale bar, 1 cm. **a**, Discrimination. *lim-6* mutants located and remained at the peak of a chloride gradient superimposed on a high background concentration (100 mM) of sodium (left) but failed to locate the peak of a sodium gradient superimposed on a high background concentration (100 mM) of chloride (right). **b**, Control. *lim-6* mutants located and remained at the peak of gradients identical to those in **a** when the background was omitted. **c**, Saturation. *lim-6* mutants failed to locate the peak of the gradient when it was superimposed on a high background concentration (100 mM) of the same ion. **d**, Average per cent time spent at the gradient peak for worms in the six conditions shown in **a–c**. Dotted line indicates mean chance performance, measured by assaying 36 mutants in plates with neither gradient nor background. Dashed line indicates the upper 95 per cent confidence interval for chance performance.

(Bonferroni post hoc comparison, $P < 0.001$), with chloride chemotaxis reduced to the chance level. These results suggest that in *lim-6* mutants ASEL is responsible, at least in part, for the persistence of chloride chemotaxis in the absence of ASER. We conclude that the *lim-6* gene is required to separate fully the sensory functions of ASEL and ASER.

The abnormal sensitivity of ASEL to chloride in *lim-6* mutants raised the possibility that the sodium pathway was altered in these worms. Indeed, we found that sodium chemotaxis was reduced in *lim-6* mutants relative to wild-type worms (Fig. 2f, S, versus Fig. 2b, S: $t = 2.12$, $P < 0.05$). This reduction appears to reflect an impairment of chemotaxis ability specific to sodium because chloride chemotaxis was actually enhanced in *lim-6* mutants relative to wild-type worms (Fig. 2e, S, versus Fig. 2a, S: $t = 2.02$, $P < 0.05$). In contrast to unilateral ablations of the ASE neurons in wild-type animals (Fig. 2b, L and R), ablation of ASEL or ASER in *lim-6* mutants produced equivalent modest, yet not significant, reductions in chemotaxis to sodium (Fig. 2f, L and R). This result suggests that in *lim-6* mutants, ASEL and ASER may have identical functions in the weakened sodium pathway. Bilateral ablation of the ASE neurons resulted in a significant reduction in sodium chemotaxis (Fig. 2f, S, versus Fig. 2f, LR: Bonferroni post hoc comparison, $P < 0.01$), indicating that ASEL and ASER remain constituents of the sodium pathway in the *lim-6* mutant. We conclude that although the constituents of the sodium pathway were not changed in *lim-6* mutants, the *lim-6* gene is required to establish the full sensitivity to sodium of ASEL. The ablation data for *lim-6* mutants are summarized in Fig. 2g, in which a strengthened chloride pathway relies on both ASEL and ASER, and a weakened sodium pathway also relies on both ASEL and ASER.

Previous experiments have shown that the G-protein-coupled receptor STR-2 is expressed in either the left or the right member of the chemosensory neuron pair AWC⁹, and that this asymmetry is necessary for behavioural discrimination in olfactory chemotaxis (P. D. Wes and C. I. Bargmann, personal communication). The fact that the *lim-6* gene is required for asymmetric expression of *gcy-5* suggests that *lim-6* may similarly be required for the behavioural discrimination between sodium and chloride ions. To test this idea, we performed a discrimination test on *lim-6* mutants under conditions identical to those in Fig. 1. We found that *lim-6* mutants could perform chemotaxis to chloride in a sodium background (Fig. 4a, d), indicating that the *lim-6* gene is not required for behavioural discrimination of chloride from sodium. In contrast, we found that *lim-6* mutants could not perform chemotaxis to sodium in a chloride background (Fig. 4a, d). Note that this effect cannot be explained by a loss of sodium sensitivity because *lim-6* mutants could perform chemotaxis to an identical sodium gradient with no background ion (Fig. 4b, d), albeit at a slightly reduced level compared with wild-type worms (Fig. 1b, d; $t = 2.12$, $P < 0.05$). Thus, the homeobox gene *lim-6* is required to discriminate sodium from chloride.

With just eight left–right homologous pairs of chemosensory neurons^{1,10–12} known to direct behavioural responses to at least 100 water soluble attractants and repellents^{7,13}, *C. elegans* faces a significant limitation in its ability to differentiate chemical stimuli. Our finding of functional asymmetries between the ASE neurons suggests that *C. elegans* has adopted the unexpected solution of increasing the effective number of different types of chemosensory neurons by breaking bilateral symmetry. Similarly, only three pairs of chemosensory neurons are known to direct responses to at least 60 volatile attractants and repellents in *C. elegans*¹⁴, and functional asymmetries have been described in one of these neuron pairs as well¹⁵. An analogous limitation may exist in the mammalian olfactory system in which hundreds of thousands of different chemical stimuli are discriminated by just 2,000 glomeruli¹⁶—the main functional units of the olfactory bulb. By analogy to *C. elegans* chemosensation, discrimination in

mammalian olfaction could be enhanced by breaking bilateral symmetry in the activation of glomeruli¹⁷. □

Methods

Chemotaxis assays

Single adult hermaphrodites were rinsed to remove OP50 bacteria and placed on a foodless, agar-filled plate for 10–40 min to accommodate, before being transferred to a second agar-filled plate in which a radially shaped gradient of attractant was established. The agar contained (in mM): CaCl₂ (1), MgSO₄ (1) and KPO₄ (25); pH 6.5. A gradient of either ammonium chloride, sodium acetate or potassium acetate was established by placing a 5- μ l drop of 1 M attractant in the centre of the assay plate at 18–24 h, and again at 3–4 h before each assay⁷. The maximum estimated attractant concentration⁶ was ~10 mM at the centre of the assay plate, and the minimum concentration was ~50 μ M at the edge of the plate. At these concentrations, neither ammonium nor acetate ions are attractive⁷. We recorded movement by noting the location of the worm's centroid at 1-s intervals for 20 min using an automated tracking system with 257 pixels mm⁻¹ resolution⁶. Each animal started 11 mm away from the gradient peak, and was tested only once.

Laser ablation of neurons

Neurons were ablated in L1 and early L2 larvae as described¹⁸. Neurons were identified for ablation by expression of green fluorescent protein (GFP) restricted to ASER by the *gcy-5* promoter, and restricted to ASEL by the *gcy-6* promoter⁴. The presence of GFP did not affect chemotaxis, because performance was identical for animals with and without GFP expression in ASE neurons (per cent time at peak: animals with GFP, 27.1 \pm 3.67, $n = 38$, versus animals without GFP, 23.15 \pm 4.55, $n = 17$; $t = 1.31$, $P > 0.05$). Ablated animals were tested for chemotaxis 2–4 d after ablation; individuals in which GFP was still visible in the target neuron after ablation were excluded from the behavioural analysis. In sham ablations, the laser was fired near the worm without killing any cells. We took two additional measures to control for nonspecific effects. First, worms in which ASE neurons were ablated were tested for chemotaxis to diacetyl, a compound sensed by a different chemosensory neuron pair, AWA^{14,19}. Diacetyl gradients were made by placing a 1- μ l drop of diacetyl (aqueous dilution 1:100) on the assay plate ~10 min before the start of each experiment. In agreement with previous results⁴, animals with unilateral and bilateral ablations of ASE neurons exhibited normal diacetyl chemotaxis (per cent time at peak: sham, 21.7 \pm 6.16, $n = 15$; ASEL ablated, 22.5 \pm 10.0, $n = 9$; ASER ablated, 20.7 \pm 7.44, $n = 12$; both ASEL and ASER ablated, 24.6 \pm 5.23, $n = 10$; $F = 0.161$, $P > 0.05$). Second, we found no difference in average instantaneous speed (used as a measure of vitality) between worms in which ASE neurons were ablated and shams (speed: ablated, 136 \pm 5.13 μ m s⁻¹, $n = 308$, versus sham, 145 \pm 7.89 μ m s⁻¹, $n = 149$; $t = 1.65$, $P > 0.05$).

Electrophysiology

Animals were prepared and dissected as described^{8,20}. We carried out whole-cell patch-clamp recordings using electrodes made from borosilicate glass tubing (Sutter BF120-69-10, Novato, CA) filled with (in mM): potassium gluconate (125), KCl (18), 4 NaCl (4), MgCl₂ (1), CaCl₂ (0.6), HEPES (10), EGTA (10); pH 7.2 with KOH. In some experiments N-methyl-D-glucamine was substituted for K⁺ in the recording pipette. External saline contained (in mM): NaCl (145), KCl (5), CaCl₂ (1), MgCl₂ (5), HEPES (10), D-glucose (20); pH 7.2 with NaOH. Membrane current was amplified with a modified Axopatch 200A (Axon Instruments, Foster City, CA), filtered at 10 kHz and digitized at 25 kHz. Voltages were corrected for liquid junction potentials. Neurons were identified by GFP expression as described above.

Data analysis

Probability density plots were made by counting the total number of visits made by a given test group to each square millimetre of the assay plate and dividing by the total number of sample intervals. Instantaneous speed was calculated by measuring the displacement of the centroid of the worm once per second. We quantified chemotaxis performance by computing the percentage of time that the centroid of the animal was within a circular region (10-mm diameter) centred at the peak of the gradient. The results presented here remained qualitatively the same when the diameter of the peak region used to calculate chemotaxis performance was increased to 20 mm (data not shown). All averages are reported \pm 95 per cent confidence intervals.

Received 7 November 2000; accepted 25 January 2001.

- Bargmann, C. I. & Horvitz, H. R. Chemosensory neurons with overlapping functions direct chemotaxis to multiple chemicals in *C. elegans*. *Neuron* **7**, 729–742 (1991).
- Ward, S., Thompson, N., White, J. & Brenner, S. Electron microscopical reconstruction of the anterior sensory anatomy of the nematode *Caenorhabditis elegans*. *J. Comp. Neurol.* **160**, 313–338 (1975).
- White, J., Southgate, E., Thompson, J. & Brenner, S. The structure of the nervous system of the nematode *Caenorhabditis elegans*. *Phil. Trans. R. Soc. Lond. B* **314**, 1–340 (1986).
- Yu, S., Avery, L., Baude, E. & Garbers, D. L. Guanylyl cyclase expression in specific sensory neurons: a new family of chemosensory receptors. *Proc. Natl Acad. Sci. USA* **94**, 3384–3387 (1997).
- Hobert, O., Tessmar, K. & Ruvkun, G. The *Caenorhabditis elegans* *lim-6* LIM homeobox gene regulates neurite outgrowth and function of particular GABAergic neurons. *Development* **126**, 1547–1562 (1999).
- Pierce-Shimomura, J. T., Morse, T. M. & Lockery, S. R. The fundamental role of pirouettes in *Caenorhabditis elegans* chemotaxis. *J. Neurosci.* **19**, 9557–9569 (1999).
- Ward, S. Chemotaxis by the nematode *Caenorhabditis elegans*: identification of attractants and analysis of the response by use of mutants. *Proc. Natl Acad. Sci. USA* **70**, 817–821 (1973).

8. Goodman, M. B., Hall, D. H., Avery, L. & Lockery, S. R. Active currents regulate sensitivity and dynamic range in *C. elegans* neurons. *Neuron* **20**, 763–772 (1998).
9. Troemel, E. R., Sagasti, A. & Bargmann, C. I. Lateral signaling mediated by axon contact and calcium entry regulates asymmetric odorant receptor expression in *C. elegans*. *Cell* **99**, 387–398 (1999).
10. Bargmann, C. I., Thomas, J. H. & Horvitz, H. R. Chemosensory cell function in the behavior and development of *Caenorhabditis elegans*. *Cold Spring Harb. Symp. Quant. Biol.* **55**, 529–538 (1990).
11. Bargmann, C. I. & Horvitz, H. R. Control of larval development by chemosensory neurons in *Caenorhabditis elegans*. *Science* **251**, 1243–1246 (1991).
12. Kaplan, J. M. & Horvitz, H. R. A dual mechanosensory and chemosensory neuron in *Caenorhabditis elegans*. *Proc. Natl Acad. Sci. USA* **90**, 2227–2231 (1993).
13. Dusenbery, D. B. Analysis of chemotaxis in the nematode by counter current separation. *J. Exp. Zool.* **188**, 41–47 (1974).
14. Bargmann, C. I., Hartwig, E. & Horvitz, H. R. Odorant-selective genes and neurons mediate olfaction in *C. elegans*. *Cell* **74**, 515–527 (1993).
15. Wes, P. D. & Bargmann, C. I. *C. elegans* odour discrimination requires asymmetric diversity in olfactory neurons. *Nature* **410**, 698–701 (2001).
16. Mori, K. & Yoshihara, Y. Molecular recognition and olfactory processing in the mammalian olfactory system. *Prog. Neurobiol.* **45**, 585–619 (1995).
17. Rubin, B. D. & Katz, L. C. Optical imaging of odorant representations in the mammalian olfactory bulb. *Neuron* **23**, 499–511 (1991).
18. Bargmann, C. I. & Avery, L. Laser killing of cells in *Caenorhabditis elegans*. *Methods Cell Biol.* **48**, 225–250 (1995).
19. Sengupta, P., Chou, J. H. & Bargmann, C. I. *odr-10* encodes a seven transmembrane domain olfactory receptor required for responses to the odorant diacetyl. *Cell* **84**, 899–909 (1996).
20. Lockery, S. R. & Goodman, M. B. Tight-seal whole-cell patch clamping of *C. elegans* neurons. *Methods Enzymol.* **295**, 201–217 (1998).

Acknowledgements

We thank C. Bargmann and P. Wes for discussions and sharing unpublished data; O. Hobert for suggesting study of the *lim-6* mutant; J. H. Thomas for technical instruction; O. Hobert, D. Garbers and The *C. elegans* Genetics Center for strains; M. Moravec and J. Cervantes for technical assistance; and J. Eisen, M. Goodman, T. Morse and M. Westerfield for discussion. This work was supported by the National Science Foundation; the National Institute of Mental Health; the National Heart, Lung, and Blood Institute; the Office of Naval Research; The Sloan Foundation; and The Searle Scholars Program.

Correspondence and requests for materials should be addressed to S.R.L. (e-mail: shawn@lox.uoregon.edu).

***C. elegans* odour discrimination requires asymmetric diversity in olfactory neurons**

Paul D. Wes & Cornelia I. Bargmann

Howard Hughes Medical Institute, Programs in Developmental Biology, Neuroscience, and Genetics, Department of Anatomy and Department of Biochemistry and Biophysics, The University of California, San Francisco, California 94143-0452, USA

Caenorhabditis elegans senses at least five attractive odours with a single pair of olfactory neurons, AWC, but can distinguish among these odours in behavioural assays¹. The two AWC neurons are structurally and functionally similar, but the G-protein-coupled receptor STR-2 is randomly expressed in either the left or the right AWC neuron, never in both². Here we describe the isolation of a mutant, *ky542*, with specific defects in odour discrimination and odour chemotaxis. *ky542* is an allele of *nsy-1*, a neuronal symmetry, or *Nsy*, mutant in which STR-2 is expressed in both AWC neurons². Other *Nsy* mutants exhibit discrimination and olfactory defects like those of *nsy-1* mutants. Laser ablation of the AWC neuron that does not express STR-2 (AWC^{OFF}) recapitulates the behavioural phenotype of *Nsy* mutants, whereas laser ablation of the STR-2-expressing AWC neuron (AWC^{ON}) causes different chemotaxis defects. We propose that odour discrimination can be achieved by segregating the detection of different odours

into distinct olfactory neurons or into unique combinations of olfactory neurons.

Caenorhabditis elegans, like other animals, detects odours with G-protein-coupled receptors such as the high-affinity diacetyl receptor encoded by the *odr-10* gene³. Individual chemosensory neurons express several receptor genes^{4,5}, potentially allowing them to detect many odours but presenting a challenge for discriminating among odours. Nevertheless, *C. elegans* does exhibit the ability to distinguish between many odours in behavioural assays: a high uniform concentration of an odour will block chemotaxis toward a point source of that odour but not toward point sources of other odours^{1,6}. The five odours sensed by the two AWC neurons— butanone, benzaldehyde, 2,3-pentanedione, isoamyl alcohol and 2,4,5-trimethylthiazole—use a common cyclic GMP signalling pathway, comprising the G_α subunit ODR-3, the transmembrane guanylyl cyclases ODR-1 and DAF-11, and the cyclic-nucleotide-gated channel TAX-2/TAX-4 (refs 1, 6–10). Overexpression of ODR-1 perturbs discrimination between butanone and benzaldehyde through mechanisms that are not understood⁶.

To gain insight into the mechanism of discrimination, we performed a genetic screen for loss-of-function mutants that cannot detect a point source of benzaldehyde in a high uniform concentration of butanone (Fig. 1a; and Methods). The most striking defect was observed in the mutant *ky542*, which exhibited a complete loss of benzaldehyde chemotaxis in the presence of a

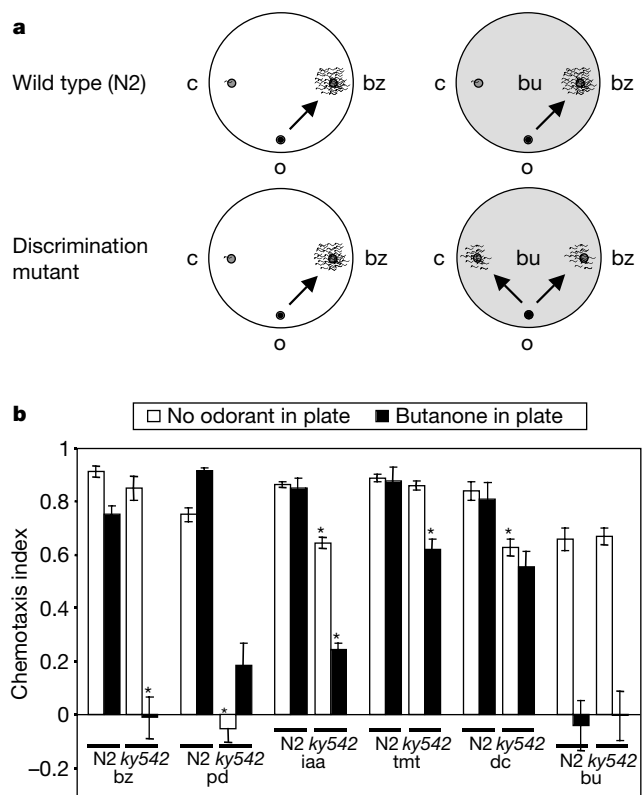


Figure 1 The *ky542* mutant has defects in olfaction and olfactory discrimination. **a**, Animals are scored for chemotaxis to a point source of benzaldehyde (bz) in the absence (chemotaxis assay, left) or presence (discrimination assay, right) of a uniform field of butanone (bu). Discrimination mutants fail to chemotax to benzaldehyde in the presence of butanone. c, control; o, origin. **b**, Population chemotaxis assays in the absence (open bars) or presence (filled bars) of butanone. Asterisks indicate statistically significant ($P < 0.001$) defects in *ky542* mutants. Genotypes and odorants are listed below each assay. N2, wild type; bu, 1:1,000 butanone; bz, 1:200 benzaldehyde; dc, 1:1,000 diacetyl; iaa, 1:100 isoamyl alcohol; pd, 1:10,000 2,3-pentanedione; tmt, 1:1,000 2,4,5-trimethylthiazole. The abbreviations are the same for all figures.